Research Article *Science, Engineering and Health Studies 2018, 12(2), 69-76*

Mapping of cloud cover from satellite data over Thailand

Doojdao Charuchittipan, Serm Janjai*, Noppamas Pratummasoot,
Sumaman Buntoung and Sahussa Peengam

Department of Physics, Faculty of Science, Silpakorn University, Nakhon Pathom 73000, Thailand
**Corresponding author: serm.janjai@gmail.com*

Received: June 21, 2017; Accepted: August 2, 2018

ABSTRACT

In this study, an empirical model for estimating cloud cover from satellite data was developed. The Skyview instruments were installed at four stations located in Chiang Mai (18.78°N, 98.98°E), Ubon Ratchathani (15.25°N, 104.87°E), Nakhon Pathom (13.82°N, 100.04°E) and Songkhla (7.20°N, 100.60°E) in order to record the images of the sky. A five-year period (2009-2013) of the cloud cover derived from the sky images and cloud index derived from MTSAT–1R satellite data were acquired. Based on these data, a model relating the cloud cover to the cloud index was formulated. To validate its performance, the model was used to calculate cloud cover at the four stations during a two-year period (2014-2015). It was found that the measured and calculated cloud cover data were in reasonable agreement with root mean square differences (RMSD) and mean bias difference (MBD) of 12.9% and 3.5%, respectively. Finally, the model was used to calculate cloud cover over Thailand and the results were shown as maps.

Keywords: Cloud cover; Model; Satellite data; Skyview

1. INTRODUCTION

Cloud comprises tiny water droplets and/or ice crystals and it is one of weather elements, which characterize a state of the atmosphere (WMO, 2014; Ahrens, 2007). Cloud observation has been part of the weather forecast process since the old days. Cloud covers more than two third of the earth's atmosphere (Stubenrauch et al., 2013), which signifies its influences on the earth's climate. For example, a cloud can interact with both shortwave and longwave radiations. Cloud reflects and absorbs solar radiation, which occupies the shortwave region, while it emits and absorbs longwave radiation in the form of infrared radiation from the atmosphere and earth's surface (Arking, 1991). Cloud is also the source of precipitations, whose formations release heat back to the atmosphere. Interactions between cloud, radiation and precipitation are all interrelated as a feedback loop, and have been in attentions by many researchers, especially in radiative and water budgets (Rossow and Schiffer, 1999; IPCC, 2013).

Due to cloud's role in the energy and water cycles, many atmospheric models such as Libradtran and SBDART require information on clouds as input parameters (Mayer et al., 1997; Paul and Shiren 1998). To obtain these parameters, it is essential to study cloud properties (Long et al., 2006). For example, Yin et al. (2015) determined cloud optical thickness by a multifilter rotating shadowband radiometer and then investigated the seasonal variation influenced from El

ISSN Online 2630-0087 DOI: https://doi.org/10.14456/sehs.2018.6

Nino and Southern Oscillation (ENSO).

One important property of cloud, which World Meteorological Organization (WMO) requires every meteorological station to measure, is total cloud amount or total cloud cover (WMO, 2014). It has been traditionally obtained by visual observation, which certainly subject to human error. Nowadays, the visual observation is replaced by many modern instruments, e.g. laser ceilometer, pyrometer and sky camera (Luo et al., 2010). Although these modern instruments can give an accurate cloud cover, they require a lot of maintenance and budget to maintain their operations. Therefore, the availability of such instruments is limited.

As a cloud image can be captured by meteorological satellite instruments, then derivation of cloud cover from satellite data is feasible. In this paper, we developed a method for estimating cloud cover using satellite data. This method was applied for Thailand, which cloud cover variation is strongly influenced by both East Asian and South Asian monsoons. Due to total cloud amount data in 84 meteorological stations throughout the country were obtained by visual observations, we expect this method would give a promising progress for weather and climate studies in Thailand.

2. METHODOLOGY

Mapping of cloud cover consists of five main steps, namely derivation of cloud cover from sky images, processing of satellite data, modeling, model validation and mapping. The details of each step are described in the following sections.

2.1 Derivation of cloud cover from sky images

Determining cloud cover from sky images was achieved from ground-based measurements using Skyviews which have been installed at four meteorological stations in Chiang Mai (18.78°N, 98.98°E), Ubon Ratchathani (15.25°N, 104.87°E), Nakhon Pathom (13.82°N, 100.04°E) and Songkhla (7.20°N, 100.60°E), for those representing Northern, Northeastern, Central and Southern regions of Thailand, respectively (Figure 1). The sky images were captured at five-minute interval and recorded into a PC harddisk. The resolution of each image is 640 × 480 pixels.

Figure 1 A map of Thailand showing the locations of the study sites and the pictorial view of the Skyviews used in this work. A, B, C and D indicate the Northern, Northeastern, Central and the Southern regions, respectively.

The sky images from the four stations during 9:00-15:00 of a five-year period (2009-2015) were collected. These data were undergone an algorithm that counts the ratio of number of pixels dominated by cloud to number of total sky pixels (Ghonima et al., 2012). Then this ratio was converted to cloud cover whose value ranges from 0 (clear sky) to 10 (overcast sky). The cloud cover data were then processed to monthly average cloud cover. To verify the performance of the algorithm, the monthly averaged cloud cover from the algorithm were compared with those obtained from visual observations during 2011-2013 in Chiang Mai and Songkhla as shown in Figure 2. The differences between these datasets can be presented by the percentage of root mean square difference relative to mean observed values (RMSD) and the percentage of mean bias difference relative to mean observed values (MBD). RMSD and MBD are defined as follows.

$$\mathrm{RMSD} = \frac{\sqrt{\dfrac{\sum_{i=1}^{N}(C_{y,i} - C_{x,i})^2}{N}}}{\dfrac{\sum_{i=1}^{N} C_{x,i}}{N}} \times 100 \qquad (1)$$

$$\mathrm{MBD} = \frac{\dfrac{\sum_{i=1}^{N}(C_{y,i} - C_{x,i})}{N}}{\dfrac{\sum_{i=1}^{N} C_{x,i}}{N}} \times 100 \qquad (2)$$

where $C_{y,i}$ is cloud cover derived from the Skyview, $C_{x,i}$ is cloud cover from the observation, i is the order of the data (i = 1, 2,…,N) and N is total number of the data.

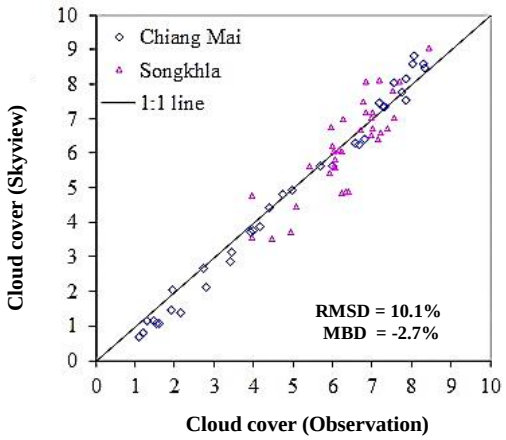

Figure 2 The comparison between monthly averaged cloud cover from Skyviews and visual observation.

The comparison result in Figure 2 shows a reasonable agreement, with RMSD and MBD of 10.1% and -2.7%, respectively.

2.2 Satellite data processing

As satellite images can depict the amount of cloud, in this study, the digital data from a visible channel (0.55-0.90 μm) of the MTSAT-1R satellite during a 10 year period (2006-2015) were used. These data covered the entire area of Thailand with a spatial resolution of 3×3 km^2. These images were transformed to the cylindrical map projection and navigated using coastlines as references. Each navigated image consists of 550×850 pixels (Figure 3), each of which has a gray level value from 0 to 255. Then the gray levels of forty-nine pixels (7×7 pixels) centered at the stations were transformed into the pseudo-reflectivity (ρ_{SAT}) by the conversion table provided by the satellite agency (JMA, 2009). In the final step, the pseudo-reflectivity was divided by the cosine of the local solar zenith angle at each pixel in order to obtain earth-atmospheric reflectivity (ρ_{EA}). This earth-atmospheric reflectivity was averaged for the forty-nine pixels centered of each station. These values will be used to estimate cloud index (n), which signify the

cloud cover, following the method of Cano et al. (1986) as:

$$n = \frac{\rho_{EA} - \rho_G}{\rho_C - \rho_G} \qquad (3)$$

where ρ_{EA}, ρ_G and ρ_C are earth–atmospheric reflectivity, ground reflectivity and maximum cloud reflectivity, respectively. The ground reflectivity (ρ_G) was estimated by using the satellite images. Monthly composite images were generated to eliminate cloud contamination. Then, these cloud-free images were converted into ground reflectivity (Janjai et al., 2006). In contrast, the maximum cloud reflectivity was estimated from the maximum value of the gray level for each pixel of satellite images all year round. Then, the satellite images with maximum value of the gray level were used to represent the maximum cloud reflectivity for each year.

From Eq. (3), when the pixel is cloud-free or $\rho_{EA} = \rho_c$, $n = 0$ and for the case of overcast condition, $\rho_{EA} = \rho_G$, $n = 1$. Additionally, for the case of party cloudy condition, $0 < n < 1$. This implies that n indicates indirectly the amount of cloud.

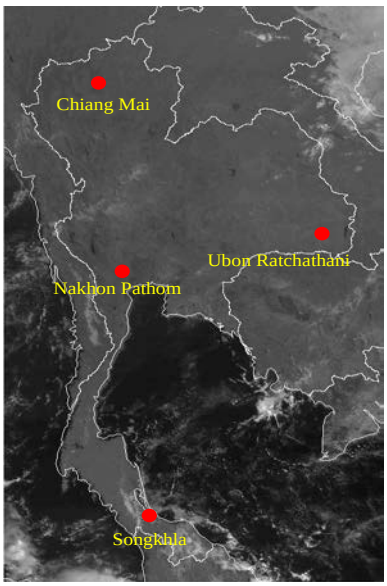

Figure 3 An example of a navigated image and the locations of the ground-based stations.

2.3 Modeling

As cloud index indicates the amount of cloud, the statistical relation between cloud index and cloud cover is expected. To obtain this relation, monthly average cloud cover from the sky images were plotted against monthly average cloud index estimated from the satellite data. These data cover the period of 2009 - 2013 and the results are shown in Figure 4.

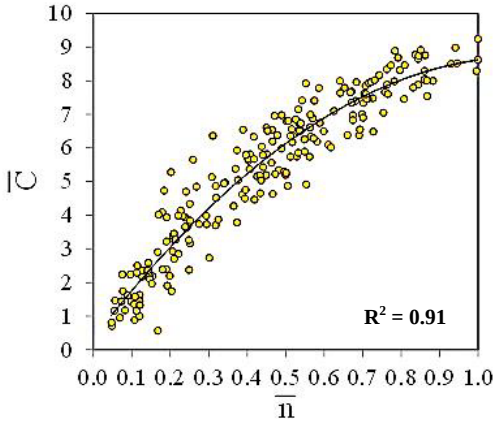

Figure 4 The relation between monthly average cloud cover from the sky images ($\bar{C}$) and monthly average cloud index ($\bar{n}$) from the satellite data.

The relation in Figure 4 was fitted by the least-square technique (Wolberg, 2006) which can be expressed as a quadratic equation:

$$\bar{C} = a_1 + a_2\bar{n} + a_3\bar{n}^2 \qquad (4)$$

where $\bar{C}$ is monthly average cloud cover, $\bar{n}$ is monthly average cloud index, and a_1, a_2 and a_3 are empirical constants. The values of these constants and their associated t-statistic are shown in Table 1.

Table 1 The empirical constants and t-statistic

Empirical constant	Value	t-statistic
a_1	0.3368	2.09913
a_2	14.896	19.74949
a_3	-6.611	-8.64677

Table 1 shows that the values of t-statistic are greater than 2, meaning that the predictor parameters in Eq. (4) are significant at 5% significance level.

2.4 Model validation

To investigate the model's performance, Eq. (4) was used to calculate cloud cover using the satellite data during 2014-2015 at the four ground-based stations in Chiang Mai, Ubon Ratchathani, Nakhon Pathom and Songkhla. The calculated cloud cover values were compared with those measured from the Skyviews. The results are depicted in Figure 5. The performance of the model is expressed in terms of RMSD and MBD as define in Eq. (1) and (2). However, in this case, $C_{y,i}$ represents cloud cover calculated from the model and $C_{x,i}$ denotes cloud cover obtained from the Skyviews. From the analysis, the values of RMSD and MBD are found to be 12.9% and 3.5%, respectively. This result implies that the model performs reasonably well in estimating the cloud cover.

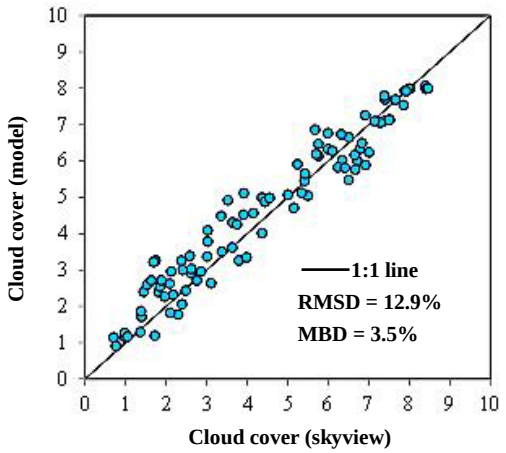

Figure 5 Comparison between cloud cover from the proposed model and that from the sky images at the four stations.

2.5 Mapping of monthly average cloud cover

After the validation, the model was used to estimate cloud cover from the cloud index derived from MTSAT-1R satellite over a period of 10 years (2006-2015) and the results are displayed as maps.

3. RESULTS AND DISCUSSION

The monthly average and yearly average maps of cloud cover of Thailand are shown in Figures 6 and 7, respectively.

Figure 6 shows monthly average cloud cover over a 10-year period (2006-2015). The seasonal variation is explicitly observed, which corresponds to several atmospheric factors, e.g. atmospheric water vapor and aerosols as well as seasonal meteorological conditions. During January to February, the Northern, the Northeastern and Central regions of Thailand has less cloud cover because the East Asian monsoon brings cold and dry air into these areas. Meanwhile, the East Asian monsoon blows moist air from the Gulf of Thailand to the Southern region, resulting in more cloud cover in this region.

Even during the calm period between March and April, cloud cover starts to show up in the lower Central Thailand. This would be caused by the trough, which spans over that area. In May, the South Asian monsoon starts to blow across the Indian Ocean and initiates the rainy season, which continues until October. This results in more cloud cover occurring over the country.

During November to December, the cloud cover distribution is quite similar to January-February as they are also under the influence of the East Asian monsoon. However, cloud cover over the Southern area is much more intensifying due to this monsoon blowing across the Gulf of Thailand.

In Figure 7, the annual average cloud cover over years 2006-2015 is presented. Since the Southern Thailand is surrounded by the sea and is influenced by both the East and South Asian monsoons, the annual average cloud cover in this region is the highest. The higher cloud cover in the western shore of the Southern Thailand is likely caused by local topography of this area. This orographic rain landscape is also found in the Eastern Thailand, which is also under the influence of the South Asian monsoon.

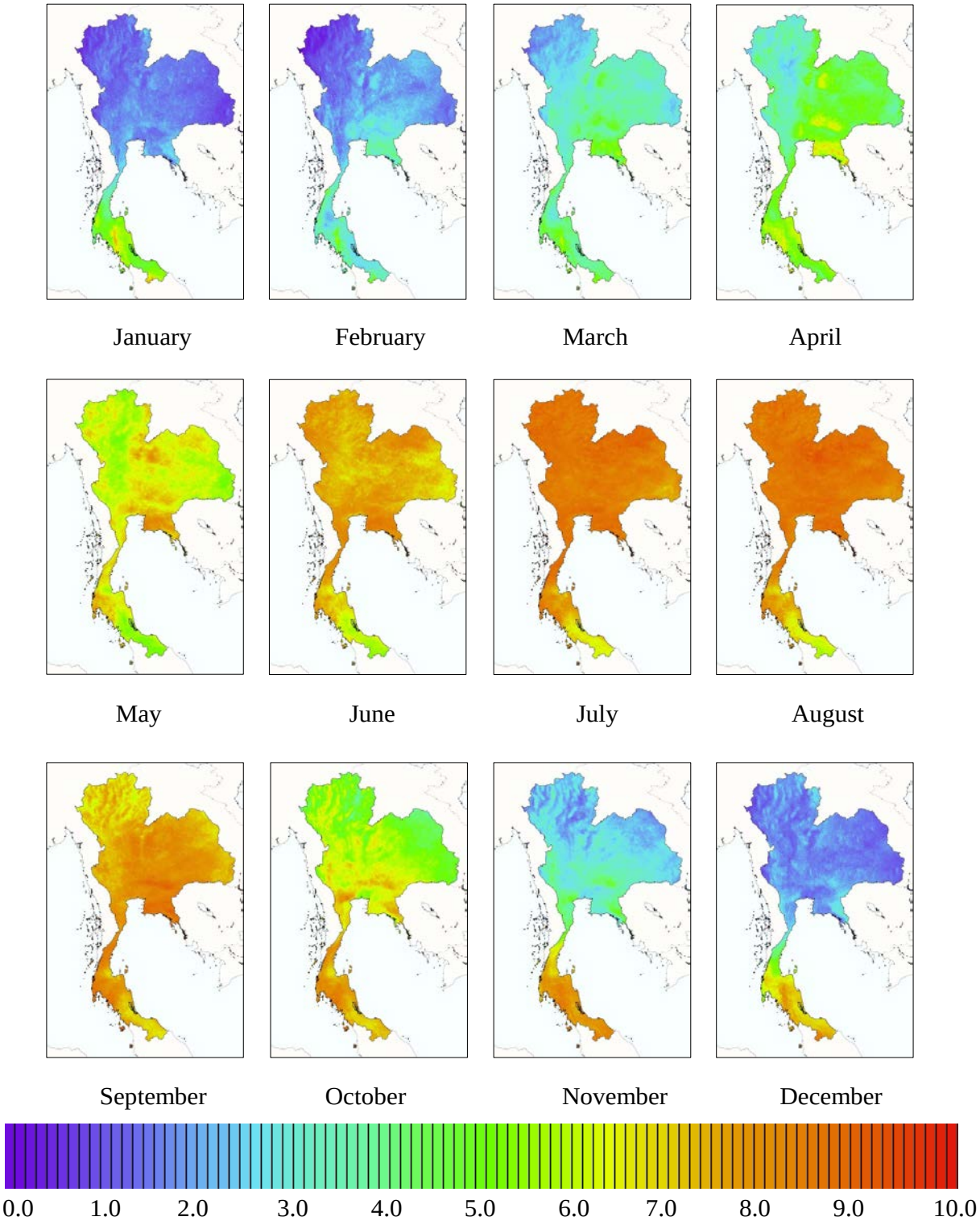

Figure 6 Monthly average cloud cover over Thailand (color code: 0 represents clear sky and 10 is completely overcast).

4. CONCLUSION

An empirical model for estimating cloud cover over Thailand from satellite data was developed. The model relates the monthly average cloud cover to the satellite-derived cloud index. This model was validated against the ground-based measurement. The cloud covers from the two datasets were in good agreement with the root mean square difference (RMSD) and the mean bias difference (MBD) of 12.9% and 3.5%, respectively. This model was used to generate long-term monthly and yearly maps of cloud cover over the region of Thailand. The maps show seasonal variation of cloud cover demonstrating the effect of monsoon and local topography over the country.

ACKNOWLEDGEMENTS

The authors are grateful to the Thailand Research Fund (TRF) for financial support as well as to Science Achievement Scholarship of Thailand (SAST) for a scholarship to the third author. Satellite data provided by the Geo-Informatics and Space Technology Development Agency (GISTDA) and cloud cover provided by Thai Meteorological Department (TMD) are highly appreciated.

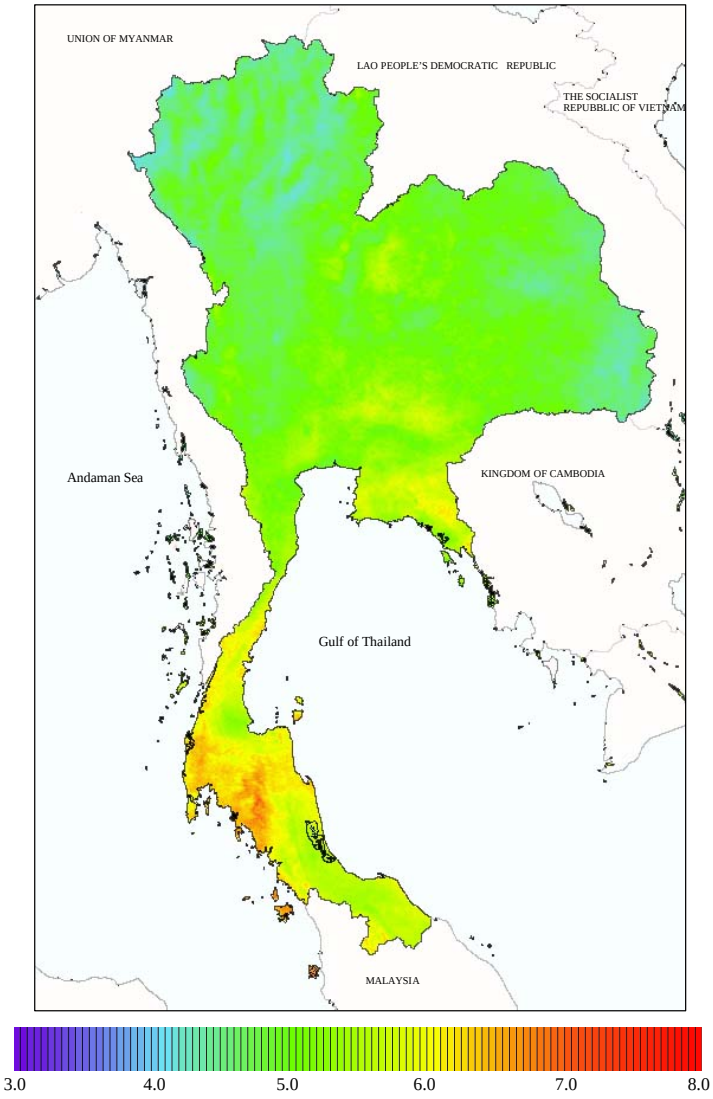

Figure 7 Long-term yearly average cloud cover over Thailand.

REFERENCES

Ahrens, C.D. (2007). Meteorological today: An introduction to weather, climate, and the environment, 9th ed., Brooks/Cole Publishing Company, Belmont, California, United States.

Arking, A. (1991). The radiative effects of clouds and their impact on climate. *Bulletin of the American Meteorological Society*, 72(6), 795-813.

Cano, D., Monget, J.M., Albuisson, M., Guillard, H., Regas, N., and Wald, L. (1986). A method for the determination of the global solar radiation from meteorological satellite data. *Solar Energy*, 37(1), 31-39.

Ghonima, M.S., Urquhart, B., Chow, C.W., Shields, J.E., Cazorla, A., and Kleissl, J. (2012). A method for cloud detection and opacity classification based on ground based sky imagery. *Atmospheric Measurement Techniques*, 5, 2881-2892.

IPCC (2013). Climate Change 2013: The physical science basis. Contribution of working group I to the fifth assessment report of the Intergovernmental Panel on Climate. Cambridge University Press.

Janjai, S., Wanvong, W., and Laksanaboonsong, J. (2006). The determination of surface albedo of Thailand using satellite data. In *Proceedings of the 2nd Joint International Conference on Sustainable Energy and Environment (SEE'06)*, Bangkok, Thailand, 156-161.

JMA, (2009). Conversion table of satellite data. Japanese Meteorological Agency, Tokyo, Japan.

Long, C.N., Sabburg, J.M., Calbo, J., and Pages, D. (2006). Retrieving cloud characteristics from ground-based daytime color all-sky images. *Journal of Atmospheric and Oceanic Technology*, 23, 633-652.

Luo, L., Hamilton, D., and Han, B. (2010). Estimation of total cloud cover from solar radiation observations at Lake Rotorua, New Zealand. *Solar Energy*, 84, 501-506.

Mayer, B., Seckmeyer, G., and A. Kylling (1997). Systematic long-term comparison of spectral UV measurements and UVSPEC modeling results. *Journal of Geophysical Research*, 102(D7), 8755-8767.

Paul, R. and Shiren, Y. (1998). SBDART: A research and teaching software tool for plane-parallel radiative transfer in the earth's atmosphere. *Bulletin of the American Meteorological Society*, 79(10), 2101-2114.

Rossow, W. B., and Schiffer, R. A. (1999). Advances in understanding clouds from ISCCP. *Bulletin of the American Meteorological Society*, 80(11), 2261-2287.

Stubenrauch, C. J., Rossow, W. B., Kinne, S., Ackerman, S., Cesana, G., Chepfer, H., Girolamo, L. D., Getzewich, B., Guignard, A., Heidinger, A., Maddux, B. B., Menzel, W. P., Minnis, P.,Pearl, C., Platnick, S., Poulsen, C., Riedi, J., Sun-Mack, S., Walther, A., Winker, D., Zeng, S., and Zhao, G. (2013). Assessment of global cloud datasets from satellites: Project and database initiated by the GEWEX Radiation Panel. *Bulletin of the American Meteorological Society*, 94(7), 1031-1049.

WMO (2014). Guide to meteorological instruments and methods of observation (WMO-No.8), World Meteorological Organization, Geneva, Switzerland.

Wolberg, J. (2006). Data analysis using the method of least squares: Extracting the most information from experiments. Springer. Berlin.

Yin, B., Li, S., Li, R., Min, Q., and Duan, M. (2015). Interannual variation of cloud optical properties at ACRF Manus and Nauru sites from MFRSR measurements. *Journal of Quantitative Spectroscopy & Radiative Transfer*, 153, 29-37.